Hindawi
Advances in Materials Science and Engineering
Volume 2022, Article ID 3177172, 8 pages
https://doi.org/10.1155/2022/3177172

Research Article

Optical Microstructure, FESEM, Microtensile, and Microhardness Properties of LM 25-B_4Cnp-Grnp Hybrid Composites Manufactured by Selective Laser Melting

M. Babu,[1] S.R. Venkataraman,[2] Putta Nageswara Rao,[3] Venkateswara Rao,[4] S. Kaliappan,[5] Pravin P Patil,[6] S. Sekar,[7] K.P. Yuvaraj,[8] and Arundeep Murugan[9]

[1]*Department of Mechanical Engineering, Easwari Engineering College, Ramapuram, Chennai, India*
[2]*Mechanical Engineering Department, S.A.Engineering College, Avadi - Poonamallee Road Veeraraghavapuram, Chennai, Tamilnadu, India*
[3]*Vasireddy Venkatadri Institute of Technology, Guntur, Andhra Pradesh, India*
[4]*Department of Mechanical Engineering, Vignana Bharathi Institute of Technology, Hyderabad, Telangana, India*
[5]*Department of Mechanical Engineering, Velammal Institute of Technology, Chennai, Tamil Nadu, India*
[6]*Department of Mechanical Engineering, Graphic Era Deemed to Be University, Bell Road Clement Town, Dehradun, Uttarakhand, India*
[7]*Department of Mechanical Engineering, Rajalakshmi Engineering College, Rajalakshmi Nagar Thandalam, Chennai, Tamilnadu, India*
[8]*Department of Mechanical Engineering, Sri Krishna College of Engineering and Technology, Coimbatore, Tamilnadu, India*
[9]*School of Mechanical and Industrial Engineering, Institute of Technology, Debre Markos University, Debre Markos, Ethiopia*

Correspondence should be addressed to Arundeep Murugan; arundeepmurugan@gmail.com

Received 15 April 2022; Accepted 16 May 2022; Published 3 June 2022

Academic Editor: V. Vijayan

The current investigation, nano-multi-powder particles, 5 and 10 wt.% boron carbide (B_4C) and graphite (Gr) are utilized as a reinforcement, and aluminium LM 25 alloy is used as a matrix. These hybrid nanocomposites were fabricated by a novel additive manufacturing method—selective laser melting. The specimen was carried out in a cylindrical size having 2 circular slots of dimension 14 and length 50 mm. The diverse SLM specimens focused on tribological properties of impact, creep, tensile, and hardness were carried out for the three specimens with same weight percentage of nanoparticles. The consequence of the reinforcement has been performed through microtensile and microhardness tests. The microtensile and microhardness properties are evaluated by microtensile test machine and Vickers hardness tester, and the specimen has been prepared as per ASTM E8 and ASTM E18 standards. Microtensile strength and hardness were augmented by the addition of B_4C and graphite nanoparticles. The tensile strength and hardness values are 668.93 MPa and 739.16 MPa, and 193VHN and 206.79VHN, respectively. The result of the microstructure study shows homogeneous dispersion of B4Cnp-Grnp in the matrix material of the LM25 alloy. The FESEM image results of the ruined surface illustrate the addition performance of ductile fracture, brittle fracture, and ploughing of reinforced material. The consequences of the research enhanced tensile and hardness properties of composite with reinforcement added.

1. Introduction

High strength, high modulus, high toughness, low deformation, and high abrasive wear resistance are highly desirable in research areas in the automobile, aerospace, defense, aviation, electronic devices, and marine industries [1, 2]. Due to their durability, augmented specific strength-stiffness, superior elevated temperature strength, enhanced wear, superior corrosion resistance, and lightweight high-strength metal matrix nanocomposites (MMNCs) can be

utilized in a spacious assortment of applications, including biomedical engineering, aerospace, and automotive [3]. Because of their superior strength-to-weight ratio, good thermal conductivity, and better wear resistance, aluminium-based metal matrix composites (AMMCs) have become widely used in automotive, infrastructure, transportation, aircraft, and defense sectors over the last two decades. It is primarily used in the production of automotive components such as connecting rods and cylinder liners [4]. The properties of nanoreinforced LM 25 aluminium alloy improved tensile strength, yield strength, elongation of the composites, and wear and corrosion resistance [5]. The processing method and processing parameters that can endow with a uniform distribution of hard/soft reinforcement and an excellent matrix-reinforcement interface, in addition to the selection of metal matrix and hard/soft reinforcement, play a critical role in the improvement of MMC properties [6].

The majority of Al-based nano- and hybrid composites that have been created are still in the research stage. Because of their better performance, these composites have a bright future. Automobiles, aeroplanes, marines, sporting goods, and other industries are expected to use these composites extensively. In the creation of nanocomposites, nanoscale reinforcement is critical. Nanocomposite utilization will become more common in the future as synthesis and manufacture of nanopowders become more economical. The capacity to develop nanostructure materials with unique macroscale qualities is a difficult feature of nano- and hybrid composite fabrication because manufacturing procedures have a significant impact on the morphology and material properties at the nanometer level [7].

B_4C might be used as a strengthening reinforcing material in the development of AMMCs for applications requiring high strength and stiffness as well as strong wear resistance. The addition of B_4C ceramic nanoparticles to an aluminium alloy matrix increases the strength, stiffness, and corrosion resistance of the material [8]. Byra Reddy and Bharathesh investigated Al6063 alloy with B_4C nanoparticles fabricated by utilized ultrasonic-assisted stir-casting process. The mechanical properties are enhanced yield strength, ultimate tensile strength, and hardness which were drastically superior and, percentage elongation diminished with ascends of the B_4C nanoparticles [9]. Manjunatha et al. explained addition of B_4C reinforcement in nanoappearance by weight (3 to 12 percent) to aluminium alloy 7075 and showed that it improves wear resistance. In addition, incorporating B4C nanoparticles, one of the hardest materials, into the aluminium matrix improves the Al7075-B4C composite's wear resistance, hardness, and strength [10]. Manohar et al. used powder metallurgical techniques to create an AA7075/B_4C/ZrC hybrid nanocomposite. The Al3BC intermetallic compound was created in the hybrid composite, and the presence of impurity layers signifies contamination of the interfaces, which impaired the hybrid composite material's mechanical capabilities. Both composites displayed agglomeration effects in microstructural examination, but the microwave treated composite had better characteristics, indicating strong and clean interfaces [11]. B_4C and industrial waste fly ash were created by Kumar et al. Stir casting was used to make reinforcement particles with an Al-Mg-Si-T6 hybrid metal matrix composite. Mechanical qualities such as tensile strength, compression strength, hardness, and density were improved as a result of this investment. A complete interfacial bonding with fewer voids was detected using an optical microscope, which impacts the improvement of mechanical characteristics [12]. Dirisenapu et al. used ultrasonic aided stir casting to manufacture aluminum 7010 HMMCs with B_4C and BN nanoparticles as reinforcing materials, mixed in equal proportions with 0 to 2.5 weight percent of nanoparticles in increments of 0.5. The percentage of elongation and impact strength of the composite are lowered with the addition of particle reinforcement up to 2 wt.% and then raised, according to the results of the tests. Although the tensile strength and microhardness increased with an increase in the weight percent of B_4C and BN particles up to 2, they thereafter decreased [13].

Sridhar and Lakshmi looked at making Al 7075-SiC-graphite hybrid composites by powder metallurgy. The wear, density, and hardness characteristics of the material were investigated. The presence of Gr and Sic in the matrix, as well as the efficacy of graphite in the matrix to decrease wear, improved the investigation's density and hardness outcomes [14]. Improved dual reinforcement nanographite and zirconium oxide (ZrO_2) with Al7075 hybrid composites were produced by Kumar et al. using a relatively easy stir casting procedure. The use of dual reinforcements boosted the hardness, impact, and tensile strength of hybrid composites. Following the addition of these reinforcements, the ductility of the Al7075 alloy somewhat decreased. When compared to the base matrix alloy Al7075, the hybrid composites had a higher wear resistance [15]. Abhishek Sharma et al., investigated the behaviour of Al6061-SiC-graphite hybrid metal grid composites that were friction stir-treated. When manufactured with the right combination of processing settings, the Al6061-SiC-graphite hybrid surface composite exhibits exceptional nanomechanical and electrochemical properties. When produced with the right set of processing conditions, the hybrid surface composite outperforms monocomposites in terms of corrosion resistance [16]. Rajkumar and Santosh used a two-step stir casting procedure to make Al-Gr and Al-NanoGr particulate MMCs. By generating a thick graphite layer at the contact surface, nanographite-reinforced aluminium composites displayed greater load bearing capacity and lower coefficient of friction than aluminium-graphite composites [17].

SLM stands for selective laser melting, and it is a powder bed fusion metal additive manufacturing technique used in the biomedical, defense, aerospace, and automotive sectors to create highly customized and value-added products. Because of its light weight, excellent strength, and corrosion resistance, aluminium alloy is one of the most commonly utilized metals in SLM components in these industries. In service, parts utilized

in such applications may be exposed to high temperatures and severe dynamic loadings. It is critical to comprehend the mechanical reaction of SLM's products under various loading and operating circumstances [18]. The corrosion and hardness characteristics of 7075 aluminium alloy manufactured using SLM were investigated by Liu et al. The findings of the microstructure examination revealed that the SLM-fabricated alloy exhibits an evident inter-channel structure. The hardness and corrosion characteristics of Al alloys are significantly improved by S-phases and θ-phases precipitated at the grain boundary [19]. Scandium-modified aluminium alloy treated by SLM 280HL was suggested by Koutny Daniel et al., and the material is well-processable with SLM, attaining densities >99% [20]. Hu et al. explored how different heat treatment procedures affected 7075 aluminium alloy produced by selective laser melting (SLM). The findings revealed contraction and porosity on the peak surface of as conventional alloys, as well as the distribution of the undissolved crude subsequent stage in the grain boundary [21]. Under solid solution plus twofold ageing, Sun et al. investigated the hardness, phase transition, and microstructure of 7075 aluminium alloy synthesized by selective laser melting (SLM). In comparison with the as-received alloy (HV80), the hardness rose with solid solution plus twice ageing, and the average hardness is now around HV158 [22]. In this present work, aluminium LM 25 alloy reinforced by nano-multi-powder particles, 5 and 10 wt.% B4Cnp and Grnp, was prepared by SLM. After that, mechanical testing such as microtensile and microhardness was carried out and improved the mechanical properties.

2. Experimental Testing and Setup

2.1. Matrix and Reinforcement Material. For the experiment, Bhoomi Metal and Alloys in Maharashtra provided Al LM25 alloy powder (60 m = 2.66 g/cc). Work material is LM 25 alloy, which is utilized in the food, chemical, and electrical sectors [23]. The predicament of reinforced particle agglomeration in AMMCs has survived as the contraption of composites and is complicated to tackle. The prevalence of agglomeration is preposterous for a variety of reasons. The particulate sizes and wettability of the border between the reinforced particles and the matrix are the most important parameters.

The following steps were taken to improve wettability: (a) increasing solid surface energies, (b) lowering matrix alloy surface tension, and (c) lowering solid/liquid interface energy [24, 25]. As a consequence, LM 25 was selected as the matrix alloy for this study.

Intelligent Materials Private Limited in Punjab and Saveer Biotech Limited in Uttar Pradesh provided B_4C powder (30m, 2.26 g/cc) and Gr powder (100m, 2.27 g/cc), respectively. Particulate is made of boron carbide, which is one of the toughest materials known. Because B_4C particles are very hard, they have sharp edges [26]. Graphite is a well-known solid lubricant that has the extra virtue of being light in weight [27]. In graphite-reinforced AMCs, graphite

Figure 1: The SLM experimental setup.

Table 1: The list of SLM process machine specifications and laser process parameters.

Fiber laser	425 W
Spot sizes	95 μm
Scan processing speed	12 m/s
Build area	280 × 280 × 365 mm
Layer thickness	20–100 μm
Platform heating	220°C

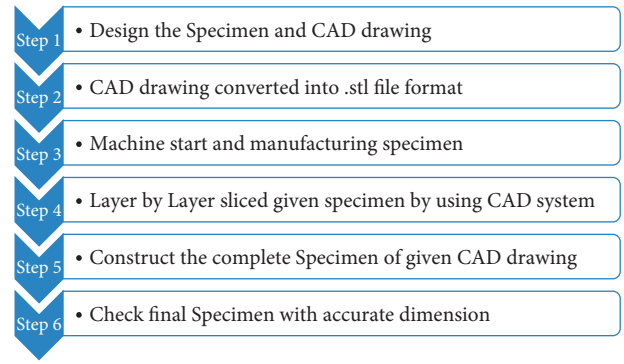

Figure 2: Working of selective laser melting (SLM) process.

functions as a solid lubricating layer between the composite and the rubbing surface, minimizing composite wear without the need of traditional solid and liquid lubricants [28]. Graphite has also been used in AMCs as hybrid reinforcement with alumina and silicon carbide, resulting in better strength and wear properties [29, 30].

2.2. Composite Preparation: SLM Process. As illustrated in Figure 1, the LM 25-B_4C-Gr specimens were made using an SLM machine designed by ARCI in Hyderabad, India. A fiber laser with a wavelength of 1076 nm is installed in an SLM machine. A continuous-wave laser with a power of 400 W and a spot size of 110 m were used throughout the whole experiment. The SLM method was carried out in vacuum to prevent the specimens from oxidizing, as reported in previous literature reviews [31–33]. The pressure in the chamber was set to 6.3×10^{-3} atmospheric pressure. Additionally, an argon gas flow was included to the experimental setup to assess the influence of ambient circumstances on make superiority. The chamber was emptied to the pressure shown above. Using argon gas to

Figure 3: Optical microscope.

Figure 5: Microhardness tester (UHL VMHT digital).

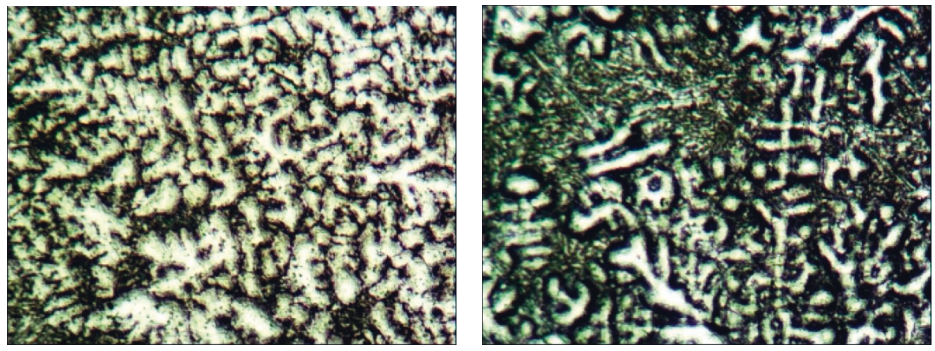

(a) (b)

Figure 4: The optical microstructure of LM 25-B_4Cnp-Grnp hybrid composites. (a) LM 25–5% B_4Cnp-5% Grnp. (b) LM 25–10% B_4Cnp-10% Grnp.

provide flow, the chamber pressure was regulated to 1.6×10^3 Pa during the laser irradiation. The process parameters and SLM technique are shown in Table 1 and Figure 2. To produce single layer samples with a dimension of 14 mm × 50 mm, the experiment was carried out with each combination of process parameters.

3. Result and Discussion

3.1. Microstructure. The SLM specimens were examined using an optical microscope, as shown in Figure 3. The samples were ground with 220 to 1000 grades of emery paper, then refined with diamond suspensions of 6, 4, and 2 mm diameters, and then imprinted with Kroll's reagent using (ASTM E407 standard) for 30 seconds to generate an accentuated discrepancy. The microstructure was studied using optical microscopy (1000x magnifications, GX51, Olympus).

At a magnification of 100, Figures 4(a) and 4(b) show the facade microstructures of LM 25-B_4Cnp-Grnp. In terms of removing particles from the surface, the LM 25-B_4Cnp-Grnp composite specimen is complex. Optical microscopes are well-known for preserving particle dispersion traces. The specimen reinforcement pattern was discovered by looking at the additive manufacturing process under an optical microscope. It was easy to see the homogeneous dispersion of B_4Cnp-Grnp in the matrix material of the LM25 alloy. The presence of B_4Cnp-Grnp causes fractures to grow, which leads to elastic deformation as load rises. Dimples, voids, clusters, and cracks characterise the LM 25-B_4Cnp-Grnp composite split. The strong interfacial connection between the reinforcements and the LM25 matrix causes fragile composite fracture in the form of fractures and rupture.

3.2. Microhardness Measurement. Microhardness measurement is a primary and important method to determine the mechanical properties of the LM 25-B_4Cnp-Grnp hybrid composites. Microhardness for the SLM samples was intended in stipulations of Vickers hardness equipment as shown in Figure 5. Enhancement of microhardness depends on the wt.% amount, dimensions, and uniform distribution of B_4C/Gr reinforcements.

Figure 6 shows the microhardness of LM 25 alloys reinforced with 5% and 10% of B_4Cnp-Grnp. The microhardness of the composite samples primarily depends on the circulation of reinforcements. Enhanced microhardness can be attained in nearly every one of the AMCs samples by inserting the B_4C/Gr particles and glowing spreading in the matrix. The microhardness values are 193VHN for 5% B4Cnp-Grnp and 206.79VHN for 10% B_4Cnp-Grnp. The results illustrated to advance the superior microhardness of the composite by using the SLM route to prepare the composites. The results are compared the previous work as listed in Table 2. The hybrid aluminium alloy composites achieved maximum hardness of 170 HV by using the fabricate ultrasonic assisted stir

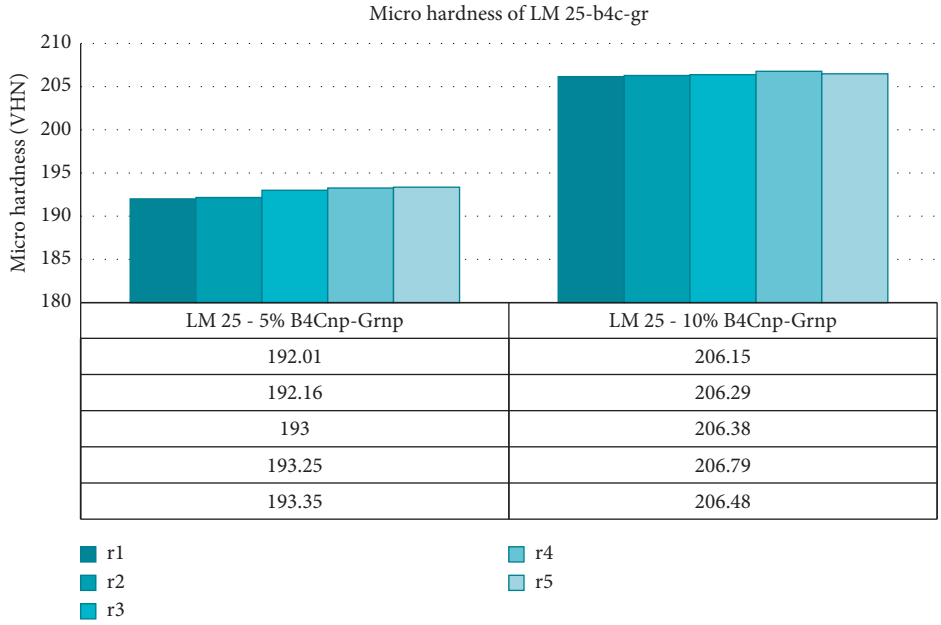

Figure 6: Microhardness values of LM 25-B4Cnp-Grnp hybrid composites.

Table 2: Research studies on LM 25- B4Cnp-Grnp hybrid composites.

Metal matrix composite	Hardness	Tensile	Composite preparation	Reference
AleMgeSi-T6/fly ash/boron carbide	62 RHN	180 MPa	Stir casting process	Saravana kumar et al., [12]
AA7075/B4C/ZrC hybrid nanocomposite	132 HV	469 MPa	Powder metallurgy techniques	Manohar.G et al., [11]
Al7010/B4C/BN	170 HV	227.089 MPa	Ultrasonic assisted stir casting technique	Gopichand dirisenapu et al., [13]
Al6063 alloy composites/B_4C	84 BHN	143 MPa	Ultrasonic assisted stir-casting process	B. Byra reddy, and T. P. Bharathesh [9]
Al2218 alloy and its nano-B4C composites	85.66 BHN	229 MPa	Stir casting process	Vidyadhar pujar et al., [34]
Nanographite and ZrO2-reinforced Al7075 alloy	75 BHN	260 Mpa	Stir casting method	Raj kumar et al., [15]
Al12Si + 10%TiN	156 HV	347 Mpa	Selective laser melting	Xaiopeng Li et al., (2022) [35]
A356/B_4C composite	77 BHN	271 Mpa	Electromagnetic stir casting process with vacuum	Shyam lal et al., (2020) [36]
Al6061-SiC-graphite hybrid surface composite	1.2 Gpa	82 Gpa	Friction stir processing	Abhishek sharma [16]
Nano- and micro-Gr/aluminium 6061 alloy	63 HRC	165 MPa	Two step stir castingtwo step stir casting	Rajkumar and santosh [17]

casting technique [13]. The present work was compared with previous works, and the mechanical properties of microhardness value are enhanced superior.

3.3. Microtensile Tests. Microtension tests are used to measure the strength of LM 25-B_4Cnp-Grnp composites under uniaxial tensile stresses in the improvement of narrative aluminium alloys for excellence control, profitable consignment acceptance testing, and structural design assistance. It was legalized in unity with ASTM E8 standards utilizing two specimens, each measuring 50 mm in length and 14 mm in diameter, as shown in Figure 7. The microtension was habitual in any appearance at atmospheric temperature, particularly the methods of determination of yield strength, yield point, elongation, tensile strength, and reduction of area. The multiuse microtensile testing machine amid submissive seize is utilized to hold the tensile specimen as shown in Figure 8.

Increased reinforcing enhanced the composites ultimate tensile strength and stress-strain, as shown in Figure 9. Table 3 shows the variation in ultimate tensile strength with AMMCs. The B_4Cnp and Grnp reinforcement's load value has been enhanced. The maximal ultimate tensile strengths are 668.93 MPa and 739.16 MPa,

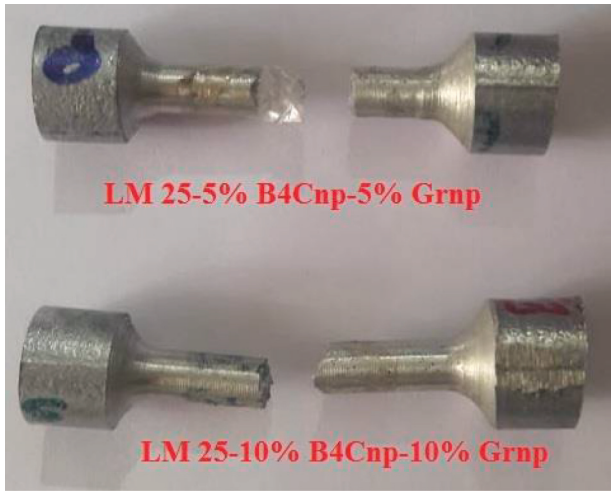

Figure 7: Microtensile test specimen.

Figure 8: Multipurpose microtensile testing machine.

respectively. In comparison with the details presented in Table 2, the tensile and hardness characteristics of the LM 25-hybrid composites have been improved by employing B_4Cnp-Grnp in addition to using different production methods, matrix materials, and reinforcement in our current research investigation.

3.4. Field Emission Scanning Electron Microscopy (FESEM). Field emission scanning electron microscopy (FESEM) is used very well in the microanalysis of LM 25-B_4Cnp-Grnp composites. It is done with colossal exaggerations, high-resolution photographs, and precise measurements of

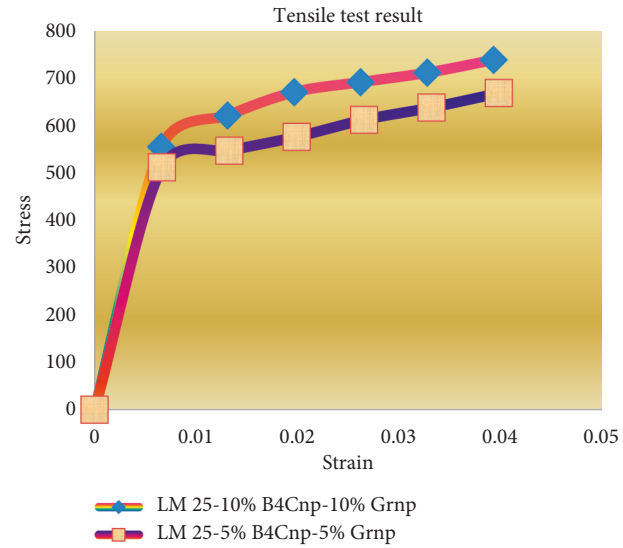

Figure 9: Microtensile test result of LM 25-B_4Cnp-Grnp hybrid composites.

Table 3: Ultimate strength value (N/mm^2).

Ultimate strength value (MPa)	
LM 25-5% B_4Cnp-5% Grnp	**668.93**
LM 25-10% B_4Cnp-10% Grnp	**739.16**

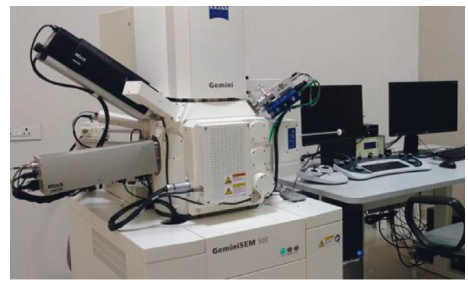

Figure 10: Field emission scanning electron microscopy (SEM).

exceedingly little face characteristics and things. SEM provides detailed high-resolution pictures of the material by focusing an electron beam over the surface and discriminating between produced and backscattered electron signals. The FESEM is shown in Figure 10.

When the manufacturers LM 25-B_4Cnp-Grnp composite material was fracture analyzed, the results are as shown in Figure 11. The mixing behavior of ductile fracture, brittle fracture, and ploughing of reinforced material can be seen in the FESEM picture of the shattered surface. Plastic deformation of the material prior to fracture causes ductile fracture behavior, which leads in the development of a hollow. Brittle fracture behaviour is caused by a fast and abrupt fracture under stress. The ploughing fracture is caused by transverse ruptures, resulting in a deep hole-like hollow. All of these indicate the mixing behaviour of the fracture.

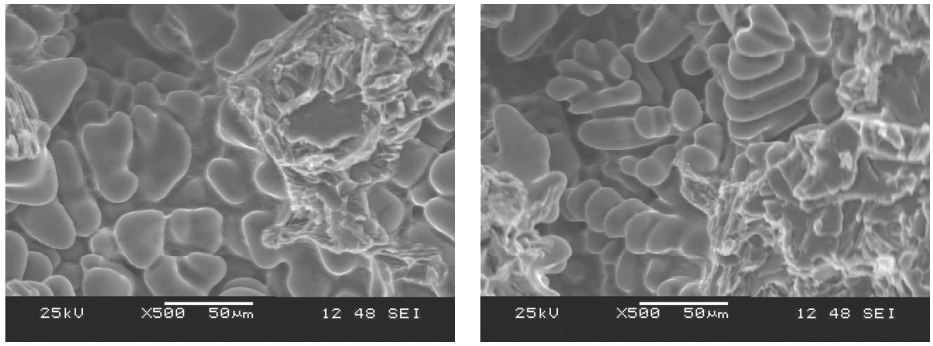

(a) (b)

Figure 11: The FESEM of LM 25-B_4Cnp-Grnp hybrid composites. (a) LM 25-5% B4Cnp-5% Grnp. (b) LM 25-10% B4Cnp-10% Grnp.

4. Conclusion

SLM has developed LM 25-B4Cnp-Grnp hybrid composites with various reinforcements (5% and 10%). The particles were equally spread throughout the matrix, according to the microstructure analysis. FESEM analysis was used to study the tensile characteristics of the LM 25-B_4Cnp-Grnp hybrid composites. The following are the results and conclusions of the microtensile and microhardness tests: according to the results of a microhardness test, the microhardness of LM 25-B_4Cnp-Grnp hybrid composites with 5% and 10% reinforcement is 193.35 VHN and 206.79 VHN, respectively, and 668.93 N/mm^2 and 739.16 N/mm^2 tensile tests of LM 25-B_4Cnp-Grnp hybrid composites, respectively. Fractographic images reveal a mixture of ductile and brittle fracture behavior, as well as reinforced material ploughing. Plastic deformation of the material prior to fracture generates ductile fracture, resulting in the creation of a hollow. A quick and abrupt fracture under stress causes brittle fracture behavior. Transverse ruptures create the ploughing fracture, which results in a deep hole-like depression [22, 37].

Data Availability

The data used to support the findings of this study are included within the article.

Conflicts of Interest

The authors declare that they have no conflicts of interest.

References

[1] S. O. Akinwamide, O. J. Akinribide, and P. A. Olubambi, "Microstructural evolution, mechanical and nanoindentation studies of stir cast binary and ternary aluminium based composites," *Journal of Alloys and Compounds*, vol. 850, Article ID 156586, 2021.

[2] A. Karthik, S. A. Srinivasan, R. Karunanithi, S. P. Kumaresh Babu, and V. K. S. Jain, "Influence of CeO2 reinforcement on microstructure, mechanical and wear behaviour of AA2219 squeeze cast composites," *Journal of Materials Research and Technology*, vol. 14, pp. 797–807, 2021.

[3] M. Malaki, W. Xu, A. Kasar et al., "Advanced metal matrix nanocomposites," *Metals*, vol. 9, no. 3, p. 330, 2019.

[4] V. Mohanavel, S. Suresh Kumar, T. Sathish, T. Adithiyaa, and K. Mariyappan, "Microstructure and mechanical properties of hard ceramic particulate reinforced AA7075 alloy composites via liquid metallurgy route," *Materials Today Proceedings*, vol. 5, no. 13, Article ID 26865, 2018.

[5] D. Yuan, K. Hu, S. Lü, S. Wu, and Q. Gao, "Preparation and properties of nano-SiCp/A356 composites synthesised with a new process," *Materials Science and Technology*, vol. 34, no. 12, pp. 1415–1424, 2018.

[6] V. Suresh, N. Hariharan, S. Paramesh, M. P. Kumar, and P. A. Prasath, "Tribological behaviour of aluminium/boron carbide (B4C)/graphite (Gr) hybrid metal matrix composite under dry sliding motion by using ANOVA," *International Journal of Materials and Product Technology*, vol. 53, no. 3/4, pp. 204–217, 2016.

[7] A. V. Muley, S. Aravindan, and I. P. Singh, "Nano and hybrid aluminum based metal matrix composites: an overview," *Manufacturing Review*, vol. 2, p. 15, 2015.

[8] S. Jayalakshmi and M. Gupta, *Metallic Amorphous Alloy Reinforcements in Light Metal Matrices*, Springer, London, United Kingdom, 2015.

[9] B. Byra Reddy and T. P. Bharathesh, "Influence of B4C nano particles on microstructure and mechanical properties of Al6063 alloy composites," in *Proceedings of the Third International Conference on Material Science, Smart Structures and Applications: (ICMSS 2020)*, Tamil Nadu, India, October 2020.

[10] T. H. Manjunatha, Y. Basavaraj, and V. Ramana, "Wear analysis of Al7075 alloyed with nano B4C: a taguchi approach," *Materials Today Proceedings*, vol. 47, pp. 2603–2607, 2021.

[11] G. Manohar, K. M. Pandey, and S. R. Maity, "Effect of microwave sintering on the microstructure and mechanical properties of AA7075/B4C/ZrC hybrid nano composite fabricated by powder metallurgy techniques," *Ceramics International*, vol. 47, no. 23, Article ID 32618, 2021.

[12] M. S. Kumar, M. Vasumathi, S. R. Begum, S. M. Luminita, S. Vlase, and C. I. Pruncu, "Influence of B4C and industrial waste fly ash reinforcement particles on the micro structural characteristics and mechanical behavior of aluminium (Al-Mg-Si-T6) hybrid metal matrix composite," *Journal of Materials Research and Technology*, vol. 15, pp. 1201–1216, 2021.

[13] G. Dirisenapu, S. P. Reddy, and L. Dumpala, "The effect of B4C and BN nanoparticles on the mechanical and microstructural properties of Al7010 hybrid metal matrix," *Materials Research Express*, vol. 6, no. 10, Article ID 105089, 2019.

[14] A. Sridhar and K. P. Lakshmi, "Evaluation of mechanical and wear properties of aluminum 7075 alloy hybrid

nanocomposites with the additions of SiC/Graphite," *Materials Today Proceedings*, vol. 44, pp. 2653–2657, 2021.

[15] R. Kumar, R. G. Deshpande, B. Gopinath, J. Harti, M. Nagaral, and V. Auradi, "Mechanical fractography and worn surface analysis of nanographite and ZrO2-reinforced Al7075 alloy aerospace metal composites," *Journal of Failure Analysis and Prevention*, vol. 21, no. 2, pp. 525–536, 2021.

[16] A. Sharma, V. Mani Sharma, B. Sahoo, J. Joseph, and J. Paul, "Study of nano-mechanical, electrochemical and Raman spectroscopic behavior of Al6061-SiC-graphite hybrid surface composite fabricated through friction stir processing," *Journal of Composites Science*, vol. 2, no. 2, p. 32, 2018.

[17] K. Rajkumar and S. Santosh, "Effect of nano and micro graphite particle on tribological performance of aluminium metal matrix composites," *Applied Mechanics and Materials*, vol. 592-594, pp. 917–921, 2014.

[18] P. Ponnusamy, R. A. Rahman Rashid, S. H. Masood, D. Ruan, S. Palanisamy, and S. Palanisamy, "Mechanical properties of SLM-printed aluminium alloys: a review," *Materials*, vol. 13, no. 19, p. 4301, 2020.

[19] P. Liu, J. Y. Hu, H. X. Li, S. Y. Sun, and Y. B. Zhang, "Effect of heat treatment on microstructure, hardness and corrosion resistance of 7075 Al alloys fabricated by SLM," *Journal of Manufacturing Processes*, vol. 60, pp. 578–585, 2020.

[20] D. Koutny, D. Skulina, L. Pantělejev et al., "Processing of Al-Sc aluminum alloy using SLM technology," *Procedia CIRP*, vol. 74, pp. 44–48, 2018.

[21] J. Y. Hu, P. Liu, S. Y. Sun, Y. H. Zhao, Y. B. Zhang, and Y. S. Huo, "Relation between heat treatment processes and microstructural characteristics of 7075 Al alloy fabricated by SLM," *Vacuum*, vol. 177, Article ID 109404, 2020.

[22] S. Sun, P. Liu, J. Hu et al., "Effect of solid solution plus double aging on microstructural characterization of 7075 Al alloys fabricated by selective laser melting (SLM)," *Optics & Laser Technology*, vol. 114, pp. 158–163, 2019.

[23] M. Senthil Kumar, M. Vanmathi, and G. Sakthivel, "SiC reinforcement in the synthesis and characterization of a356/AL2O3/sic/gr reinforced composite- paving a way for the next generation of aircraft applications," *Silicon*, vol. 13, no. 8, pp. 2737–2744, 2020.

[24] T. Xu, G. Li, M. Xie et al., "Microstructure and mechanical properties of in-situ nano γ-Al2O3p/A356 aluminum matrix composite," *Journal of Alloys and Compounds*, vol. 787, pp. 72–85, 2019.

[25] B. C. Pai, G. Ramani, R. M. Pillai, and K. G. Satyanarayana, "Role of magnesium in cast aluminium alloy matrix composites," *Journal of Materials Science*, vol. 30, no. 8, pp. 1903–1911, 1995.

[26] P. R. Jadhav, M. Nagaral, S. Rachoti, and J. I. Harti, "Impact of boron carbide and graphite dual particulates addition on wear behavior of A356 alloy metal matrix composites," *J Met Mater Miner*, vol. 30, no. 4, pp. 106–112, 2020.

[27] A. Baradeswaran and A. E. Perumal, "Study on mechanical and wear properties of Al 7075/Al2O3/graphite hybrid composites," *Composites Part B: Engineering*, vol. 56, pp. 464–471, 2014.

[28] P. Ravindran, K. Manisekar, R. Narayanasamy, and P. Narayanasamy, "Tribological behaviour of powder metallurgy-processed aluminium hybrid composites with the addition of graphite solid lubricant," *Ceramics International*, vol. 39, no. 2, pp. 1169–1182, 2013.

[29] K. Palanikumar and A. Muniaraj, "Experimental investigation and analysis of thrust force in drilling cast hybrid metal matrix (Al–15%SiC–4%graphite) composites," *Measurement*, vol. 53, pp. 240–250, 2014.

[30] V. Suresh, A. D. Praneet, and J. Anoop, "Ingenious analysis on machining parameters of aluminium alloy (LM25)/graphite (Gr)/boron carbide (B4C) hybrid composites using wire electrical discharge machining (WEDM)," *Materials Today Proceedings*, vol. 37, pp. 3112–3117, 2021.

[31] L. Poovazhagan, K. Kalaichelvan, and T. Sornakumar, "Processing and performance characteristics of aluminum-nano boron carbide metal matrix nanocomposites," *Materials and Manufacturing Processes*, vol. 31, no. 10, pp. 1275–1285, 2015.

[32] S. Arif, B. Jamil, M. B. Naim Shaikh et al., "Characterization of surface morphology, wear performance and modelling of graphite reinforced aluminium hybrid composites," *Engineering Science and Technology, an International Journal*, vol. 23, no. 3, pp. 674–690, 2020.

[33] B. Guntreddi and A. Ghosh, "Anti-frictional role of diamond and graphite suspended bio-oil based nano-aerosols at sliding interface of Al-SiCp and WC-6Co," *Tribology International*, vol. 153, Article ID 106596, 2021.

[34] V. Pujar, H. K. Srinivas, and M. Nagaral, "Processing and mechanical characterization of nano B4C particulates reinforced Al2218 alloy composites," *International Journal of Advanced Mechanical Engineering*, vol. 8, no. 1, pp. 117–126, 2018.

[35] X. Li, L. Astfalack, P. Drew, Y. Schliwa, and T. B. Sercombe, "Selective laser melting of aluminium metal matrix composites," *Proceedings of the 2nd International Conference on Progress in Additive Manufacturing*, vol. 31, no. 2, pp. 433–438, 2016.

[36] S. Lal, A. kumar, S. Kumar, and N. Gupta, "Characterization of A356/B4C composite fabricated by electromagnetic stir-casting process with vacuum," *Materials Today Proceedings*, vol. 34, pp. 832–841, 2021.

[37] S. Dhanalakshmi and T. Rameshbabu, "Comparative study of parametric influence on wet and dry machining of LM 25 aluminium alloy," *Materials Today Proceedings*, vol. 39, pp. 48–53, 2021.